PHYSICAL REVIEW B **78**, 100506(R) (2008)

Lattice and magnetic instabilities in $CaFe_2As_2$: A single-crystal neutron diffraction study

A. I. Goldman,[1,2] D. N. Argyriou,[3] B. Ouladdiaf,[4] T. Chatterji,[5] A. Kreyssig,[1,2] S. Nandi,[1,2] N. Ni,[1,2] S. L. Bud'ko,[1,2] P. C. Canfield,[1,2] and R. J. McQueeney[1,2]

[1]*Department of Physics and Astronomy, Iowa State University, Ames, Iowa 50011, USA*

[2]*Ames Laboratory, US DOE, Iowa State University, Ames, Iowa 50011, USA*

[3]*Helmholtz-Zentrum Berlin für Materialien und Energie, 100 Glienicker Strasse, D-14109 Berlin, Germany*

[4]*Institute Laue-Langevin, 38042 Grenoble Cedex, France*

[5]*Forschungszentrum Jülich Outstation, Institute Laue-Langevin, 38042 Grenoble Cedex, France*

(Received 11 July 2008; published 16 September 2008)

Neutron diffraction measurements of a high-quality single crystal of $CaFe_2As_2$ are reported. A sharp transition was observed between the high-temperature tetragonal and low-temperature orthorhombic structures at T_S=172.5 K (on cooling) and 173.5 K (on warming). Concomitant with the structural transition, the Fe moments order in a commensurate antiferromagnetic structure with a saturated moment of $0.80(5)\mu_B$/Fe directed along the orthorhombic *a* axis. The hysteresis of both the structural and magnetic transitions is 1 K between cooling and warming, consistent with previous thermodynamic, transport, and single-crystal x-ray studies and provides clear evidence of the coupling between the structural and magnetic transitions in this material.

DOI: 10.1103/PhysRevB.78.100506 PACS number(s): 75.25.+z, 75.50.Ee, 75.40.Cx

The excitement generated by the discovery of superconductivity at temperatures above 30 K in the doped iron arsenide compounds[1–4] continues to spur further research around the world. Much of this work is directed toward elucidating the underlying pairing mechanism and its relationship to anomalies in thermodynamic and transport data associated with structural and/or magnetic transitions between 100 and 200 K found in the "parent compounds" *R*FeAsO (*R*=rare earth) and AFe_2As_2 (*A*=Ba, Sr, Ca).[4–9] An apparent prerequisite for superconductivity in both classes of iron arsenides is the elimination of these higher-temperature transitions through doping with fluorine for oxygen in the former compound and potassium or sodium for the *A* ion in the latter. The introduction of different chemical species, however, adds further complexity since a range of effects (e.g., chemical disorder and doping inhomogeneities) must be considered.

In $CaFe_2As_2$, recent discoveries[10] show that: (i) under modest hydrostatic pressure, the first-order structural phase transition can be suppressed; (ii) over a limited pressure range, superconductivity occurs; and (iii) at higher pressures superconductivity can again be suppressed with the stabilization of a potentially different high-temperature phase. Pressure provides a valuable new parameter for tuning the behavior of these fascinating compounds. Further, these observations support the notion of a strong interaction between lattice and magnetic degrees of freedom and superconductivity in the AFe_2As_2 family. For example, strong spin fluctuations due to magnetic frustration in the doped compounds may play an important role for superconductivity. The importance of frustration as a mechanism for driving structural transformations in the parent phases and for supporting spin fluctuations in the superconducting phases has been discussed in several papers.[11,12] In addition, Fermi-surface nesting features apparent from band-structure calculations may give rise to magnetoelastic coupling leading to charge-/spin-density wave transitions.[13]

Several groups have used powder- and/or single-crystal diffraction to study the structural transition in $BaFe_2As_2$,[8,14,15] $SrFe_2As_2$,[16–18] $EuFe_2As_2$,[18] and $CaFe_2As_2$,[19] which is quite similar in nature to the corresponding structural transformation observed in the undoped *R*FeAsO compounds. For the AFe_2As_2 series, the high-temperature tetragonal ($I4/mmm$) structure transforms to an orthorhombic ($Fmmm$) unit cell rotated at 45° with respect to the tetragonal basal plane axes. The structural transition appears discontinuous, is often hysteretic, and coexistence is generally observed between the high-temperature tetragonal and the lower-symmetry orthorhombic phases close to the structural transformation: all hallmarks of a first-order transition. Studies of the magnetic ordering that arises in the vicinity of the structural transformation in the undoped iron arsenides have been accomplished using neutron powder-diffraction and Mössbauer measurements. In contrast to the behavior observed for the undoped iron oxypnictides,[20] powder neutron diffraction from $BaFe_2As_2$ (Ref. 14) and $SrFe_2As_2$ (Ref. 17) shows that the magnetic ordering appears to be concomitant with the structural distortion. The magnetic ordering is signaled by a sharp discontinuous transition for $SrFe_2As_2$ as measured by Mössbauer spectroscopy.[17] For $BaFe_2As_2$, however, the magnetic order parameter measured by powder neutron diffraction appears continuous. Although the coincidence in temperature of the structural and magnetic transitions argues strongly for coupling between the lattice and spin degrees of freedom in these phases, further work intent on clarifying the nature of these transitions and the relationship between them is required to develop a full picture.

Previous neutron-scattering measurements of the structural and magnetic anomalies in these compounds have been based on powder diffraction, rather than single-crystal studies, leading to some ambiguities in the details of the magnetic structure and moment direction.[14] For the lower-symmetry orthorhombic structure, single-crystal studies

allow an unambiguous determination of the magnetic structure, including the direction of the magnetic moment and the magnetic propagation vector with respect to the orthorhombic unit cell. Investigations of the structural and magnetic transitions in $CaFe_2As_2$, particularly in light of its behavior under pressure, can provide important insight into the nature of the structural and magnetic transitions.

For the neutron diffraction measurements, single crystals of $CaFe_2As_2$ were grown out of a Sn flux using conventional high-temperature solution growth techniques described previously.[19] A 7 mg single crystal with dimensions of approximately $3\times2\times0.2$ mm^3 was selected for the neutron diffraction measurements. X-ray and neutron Laue measurements confirmed the quality of the sample (mosaic $\approx0.5°$ full width at half maximum) and that the tetragonal c axis is perpendicular to the flat plate-shaped crystal surface. The neutron diffraction experiment was performed on the four-circle station D10 at the Institute Laue-Langevin using a wavelength of 2.36 Å and a two-dimensional area detector mounted on the scattering arm for data collection. A pyrolitic graphite filter was employed to reduce the higher harmonic content to $<10^{-4}$ of the primary beam energy. The sample was mounted on the cold finger of a He flow cryostat, which provided a temperature stability of 0.1 K.

We first describe the chemical and magnetic structures above and below the transition temperature T_S. For temperatures above $T_S\approx173$ K, the crystal structure of $CaFe_2As_2$ is well described by the same tetragonal structure as its sister compounds, $SrFe_2As_2$ and $BaFe_2As_2$, but with lattice constants $a_{\mathrm{Tet}}=3.879(3)$ Å and $c_{\mathrm{Tet}}=11.740(3)$ Å at $T=300$ K. Figure 1(a) shows longitudinal scans taken through the allowed nuclear $(1\ -1\ -2)$ reflection for the tetragonal structure. For reference, Fig. 1(a) also shows a scan through the position where the magnetic peak is found in the low-temperature orthorhombic phase. As the sample was cooled below T_S, Fig. 1(b) shows that the nuclear peak splits, signaling the transition to the orthorhombic phase with $a_{\mathrm{Orth}}=5.506(2)$ Å, $b_{\mathrm{Orth}}=5.450(2)$ Å, and $c_{\mathrm{Orth}}=11.664(6)$ Å at $T=10$ K. For the orthorhombic structure we employ indices $(H\ K\ L)$ for the reflections based on the relations $H=h-k$, $K=h+k$, and $L=l$, where $(h\ k\ l)$ are the corresponding Miller indices for the tetragonal phase. For example, the $(1\ -1\ -2)$ tetragonal peak is properly labeled as the orthorhombic $(2\ 0\ -2)$ peak below the structural transition. The other peak, $(0\ 2\ -2)'$, evident in Fig. 1(b) arises from the same twinning processes previously described in detail for $YBa_2Cu_3O_{7-\delta}$.[21] Indeed, two, three, or four reflections associated with twinning are observed at the nuclear positions depending on the setting of the scattering plane relative to the resolution function of the instrument.[22] However, for the lower symmetry of the orthorhombic cell, twinning produces domains along a given direction that are not equivalent and, typically, the magnetic propagation vector is aligned along a unique direction in each of the twin domains. Fig. 1(c) plots all of these peaks as functions of both Q and ω (sample rotation angle in the scattering plane) to further clarify the relationship between the twinned domains and the magnetic peak (the Q scans displayed above these plots represent a projection of the Q-ω plane on the Q axis). By comparing the position of the magnetic peak on the right side of Fig. 1(b), with the positions of the structural peaks on the left side of Fig. 1(b), we see that the magnetic peak is properly labeled as the $(1\ 0\ -1)$ magnetic reflection. More specifically, the magnetic peak appears at a position that is at half the wave vector and the same ω as the $(2\ 0\ -2)$ nuclear peak.

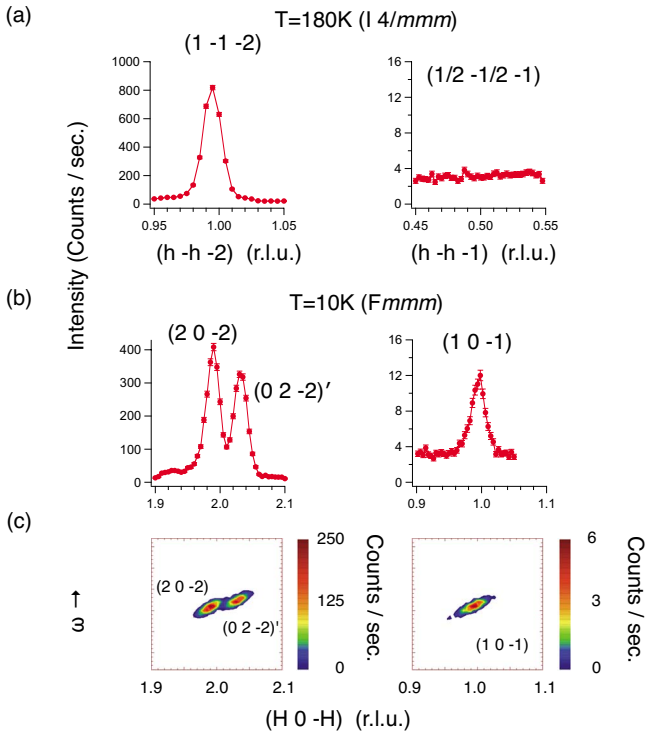

FIG. 1. (Color online) (a) Q scans through the positions of the tetragonal $(1\ -1\ -2)$ nuclear peak (referenced to the tetragonal unit cell) and the magnetic peak positions at 180 K. No intensity is observed at the positions of the magnetic reflections. (b) Below the tetragonal-to-orthorhombic transition, two twin domains are observed in longitudinal scans through the $(2\ 0\ -2)$ (indexed to the orthorhombic cell) nuclear peak position. The magnetic peak $(1\ 0\ -1)$ is associated with only one of these domains. (c) Two-dimensional plots showing the Q and ω (sample rotation in the scattering plane) dependences of peaks in (b).

At low temperature ($T=10$ K) a set of nuclear reflections and magnetic peaks was collected for refinement of the chemical and magnetic structures using FULLPROF, taking proper account of the twinning described above. The chemical unit cell below T_S is well described by the orthorhombic structure $Fmmm$ with $z_{\mathrm{As}}=0.3664(5)$ for As in the $4e$ sites. Refinement of the magnetic structure with a magnetic propagation vector of (0 1 0) (Ref. 23) yielded an ordered Fe moment of $0.80(5)\mu_B$/Fe directed along the longer orthorhombic a axis. The size and direction of the Fe moment were determined from a least-squares fit of 35 magnetic peak positions giving an acceptable fit ($R=8.8\%$) in light of the size of the crystal and magnetic moment.[25] A refinement of the magnetic structure using a model with the Fe moments directed along the shorter b axis provided poor fits ($R=84\%$) to our single-crystal data. The results of the magnetic structural refinement for the magnetic structure and moment direction of $CaFe_2As_2$ are illustrated in Fig. 2. The magnetic cell is the same as the chemical unit cell and the moments are

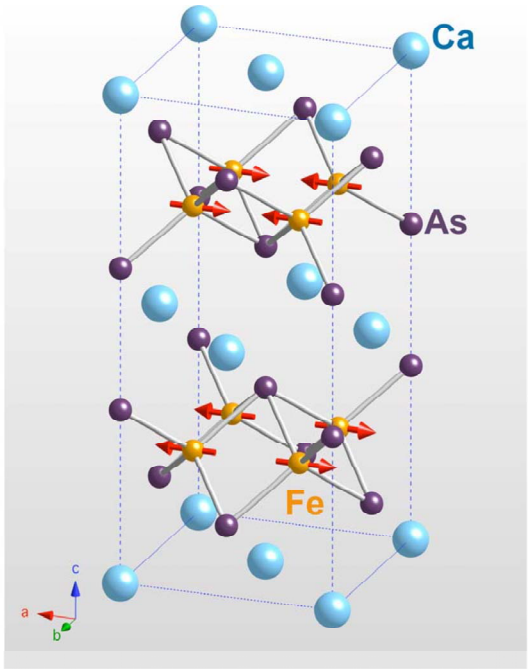

FIG. 2. (Color online) Illustration of the antiferromagnetic structure of $CaFe_2As_2$ below T_S. The magnetic unit cell is the same as the orthorhombic chemical unit cell. Fe moments are oriented along the orthorhombic a axis.

ferromagnetically coupled along the b direction and antiferromagnetically coupled along the a and c directions.

The most interesting aspect of these measurements deals with the behavior of the magnetic and structural orders close to the transition temperature T_S illustrated in Fig. 3. Figure 3(a) plots the temperature dependences of both the orthorhombic splitting of the nuclear peak and the intensity of the magnetic peak (normalized to the volume fraction of the magnetic orthorhombic phase) upon warming and cooling through the transition. Here we see that the structural transition, as measured by the orthorhombic splitting, is discontinuous over a temperature range of less than 0.5 K. Figure 3(b) plots the observed intensities of the magnetic (−1 0 1) peak and the orthorhombic (400) nuclear peak on cooling through the transition region where there is coexistence between the low-temperature antiferromagnetic orthorhombic and high-temperature tetragonal phases. The volume fraction of the orthorhombic phase was calculated from fits to the composite (400)/(040) orthorhombic and (220) tetragonal peaks in this temperature range. Whereas the magnetic ordering appears to evolve continuously over this coexistence regime [Fig. 3(b)], normalizing these data by the orthorhombic phase volume fraction, which increases in the same manner with temperature, shows that the magnetic transition is, indeed, discontinuous at the structural transition [Fig. 3(a)]. Figure 3(a) also displays a clear signature of hysteresis in the tetragonal-to-orthorhombic transformation over a range of approximately 1 K. Perhaps most interesting, however, is that the magnetic ordering shows this same hysteresis upon cooling and warming, clearly demonstrating that the structural transition and magnetic ordering are intimately connected.

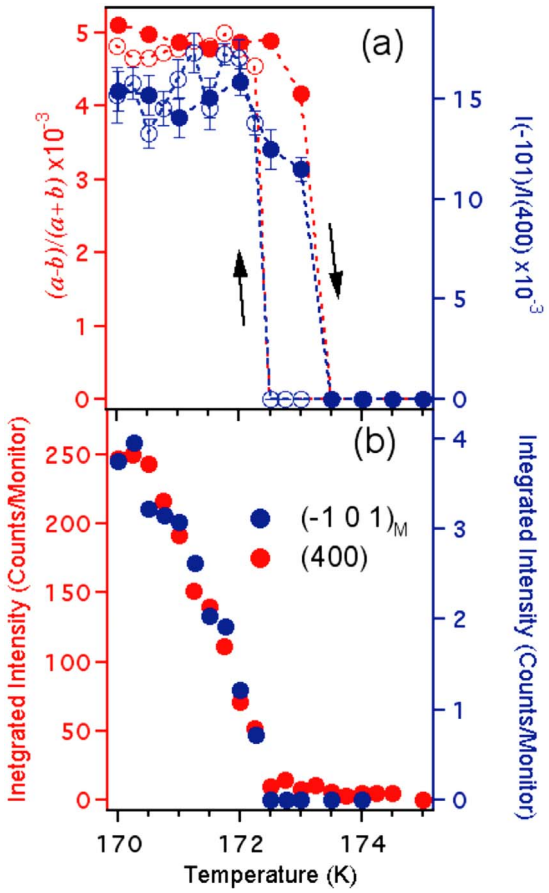

FIG. 3. (Color online) (a) Temperature dependence of the orthorhombic splitting (red curves) and magnetic integrated intensity (blue symbols) normalized to the orthorhombic volume fraction upon warming (filled circles) and cooling (open circles) through the transition. Below 170 K, both the orthorhombic distortion and the magnetic peak intensity are saturated. The dashed lines are guides to the eye. (b) The raw integrated intensities of the magnetic (−1 0 1) reflection (blue symbols) and the orthorhombic (400) nuclear peak.

It is useful at this point to compare these results with those for the magnetic structures of $SrFe_2As_2$ and $BaFe_2As_2$. Whereas the magnetic structure for $CaFe_2As_2$ is consistent with that proposed for $BaFe_2As_2$, the powder measurements on the latter system could provide only a representational solution of the magnetic structure rather than a unique ordering scheme (propagation vector and moment direction) with respect to the orthorhombic unit cell.[14] Therefore, it remains possible that the details of the magnetic structure for $BaFe_2As_2$ are different from what we have found for $CaFe_2As_2$. Interestingly, the structural transition for $BaFe_2As_2$ appears to be of first order and the magnetic ordering appears to be continuous, although the relative volume fraction of the antiferromagnetic orthorhombic phase in the coexistence region was not taken into account in those measurements. The magnetic structure determined from high-resolution magnetic powder data for $SrFe_2As_2$ by Jesche *et al.*[17] is consistent with the present single-crystal measurements on $CaFe_2As_2$. Indeed, the ordered moments determined for all three members of the AFe_2As_2

(A=Ba, Sr, Ca) are closely similar and larger than those determined for Fe in the RFeAsO (R=rare earth) compounds. The temperature dependence of the magnetic ordering in $SrFe_2As_2$, as determined by Mössbauer spectroscopy, also indicates that both the structural and magnetic orderings are discontinuous at the transition as found in this present single-crystal neutron diffraction study.

The results presented here clarify two important issues for $CaFe_2As_2$, in particular, and the AFe_2As_2 family of compounds in general: (i) They elucidate the complex nature of the $\approx$173 K phase transition seen at ambient pressure in $CaFe_2As_2$ and (ii) they provide a fixed point for speculation about the effects of pressure on this intriguing compound. Although it is true that the proximity of the magnetic and structural transitions supports the notion of coupling between the transitions, the fact that we observe [Fig. 3(a)] the same hysteresis for both the magnetic ordering and structural phase transition unambiguously links these two phase transitions at ambient pressure. The magnetic and structural phase transitions are indeed strongly coupled in $CaFe_2As_2$. This observation of such strong coupling, though, does bring up the bedeviling question of which transition, magnetic or structural, is driving the other. As shown in Ref. 10, when hydrostatic pressure is applied, the signature of the high-temperature phase transition becomes more second orderlike and finally disappears near 5 kbar close to the pressure about which a superconducting dome is centered for $T<12$ K. For even higher pressures a different resistive anomaly, which is one more commonly associated with a loss of spin disorder scattering and the onset of antiferromagnetism without any gapping of the Fermi surface, is observed. We anticipate that neutron scattering on $CaFe_2As_2$ under hydrostatic pressure will further clarify the relationship between these transitions as it appears likely that, for pressures larger than 5 kbar, at least one of them (most likely the structural one) will be fully suppressed.

Note added. Recently we became aware of a single-crystal neutron diffraction measurement on $SrFe_2As_2$, which finds the same magnetic structure and ordered moment as we described here.[24,25]

Work at the Ames Laboratory was supported by the U.S. Department of Energy–Basic Energy Sciences under Contract No. DE-AC02-07CH11358. We gratefully acknowledge the ILL for their rapid allocation of time and their support for this work. The authors would like to thank G. McIntyre for his assistance in identifying the twinning scheme.

[1] Y. Kamihara, T. Watanabe, M. Hirano, and H. Hosono, J. Am. Chem. Soc. **130**, 3296 (2008).
[2] H. Takahashi, K. Igawa, K. Arii, Y. Kamihara, M. Hirano, and H. Hosono, Nature (London) **453**, 376 (2008).
[3] X. H. Chen, T. Wu, G. Wu, R. H. Liu, H. Chen, and D. F. Fang, Nature (London) **453**, 761 (2008).
[4] M. Rotter, M. Tegel, and D. Johrendt, Phys. Rev. Lett. **101**, 107006 (2008).
[5] G. F. Chen, Z. Li, G. Li, W. Z. Hu, J. Dong, X. D. Zhang, P. Zheng, N. L. Wang, and J. L. Luo, Chin. Phys. Lett. **25**, 3403 (2008).
[6] K. Sasmal, B. Lv, B. Lorenz, A. M. Guloy, F. Chen, Y.-Y. Xue, and C.-W. Chu, Phys. Rev. Lett. **101**, 107007 (2008).
[7] G. Wu, R. H. Liu, H. Chen, Y. J. Yan, T. Wu, Y. L. Xie, J. J. Ying, X. F. Wang, D. F. Fang, and X. H. Chen, arXiv:0806.1459 (unpublished).
[8] M. Rotter, M. Tegel, D. Johrendt, I. Schellenberg, W. Hermes, and R. Pöttgen, Phys. Rev. B **78**, 020503(R) (2008).
[9] C. Krellner, N. Caroca-Canales, A. Jesche, H. Rosner, A. Ormeci, and C. Geibel, Phys. Rev. B **78**, 100504(R) (2008).
[10] M. S. Torikachvili, S. L. Bud'ko, N. Ni, and P. C. Canfield, Phys. Rev. Lett. **101**, 057006 (2008).
[11] T. Yildirim, Phys. Rev. Lett. **101**, 057010 (2008).
[12] Q. Si and E. Abrahams, Phys. Rev. Lett. **101**, 076401 (2008).
[13] I. I. Mazin, D. J. Singh, M. D. Johannes, and M. H. Du, Phys. Rev. Lett. **101**, 057003 (2008).
[14] Q. Huang, Y. Qiu, W. Bao, M. A. Green, J. W. Lynn, Y. C. Gasparovic, T. Wu, G. Wu, and X. H. Chen, arXiv:0806.2776 (unpublished).
[15] N. Ni, S. L. Bud'ko, A. Kreyssig, S. Nandi, G. E. Rustan, A. I. Goldman, S. Gupta, J. D. Corbett, A. Kracher, and P. C. Canfield, Phys. Rev. B **78**, 014507 (2008).
[16] J.-Q. Yan, A. Kreyssig, S. Nandi, N. Ni, S. L. Bud'ko, A. Kracher, R. J. McQueeney, R. W. McCallum, T. A. Lograsso, A. I. Goldman, and P. C. Canfield, Phys. Rev. B **78**, 024516 (2008).
[17] A. Jesche, N. Caroca-Canales, H. Rosner, H. Borrmann, A. Ormeci, D. Kasinathan, K. Kaneko, H. H. Klauss, H. Luetkens, R. Khasanov, A. Amato, A. Hoser, C. Krellner, and C. Geibel, arXiv:0807.0632 (unpublished).
[18] M. Tegel, M. Rotter, V. Weiss, F. M. Schappacher, R. Pöttgen, and Dirk Johrendt, arXiv:0806.4782 (unpublished).
[19] N. Ni, S. Nandi, A. Kreyssig, A. I. Goldman, E. D. Mun, S. L. Bud'ko, and P. C. Canfield, Phys. Rev. B **78**, 014523 (2008).
[20] C. de la Cruz, Q. Huang, J. W. Lynn, J. Li, W. Ratcliff II, J. L. Zarestky, H. A. Mook, G. F. Chen, J. L. Luo, N. L. Wang, and P. Dai, Nature (London) **453**, 899 (2008).
[21] G. J. McIntyre, A. Renault, and G. Collin, Phys. Rev. B **37**, 5148 (1988).
[22] G. J. McIntyre and A. Renault, Physica B **156-157**, 880 (1989).
[23] A. S. Wills, Physica B **276-277**, 680 (2000); The (010) and (101) propagation vectors are related by the allowed translation of [111].
[24] J. Zhao, W. Ratcliff II, J. W. Lynn, G. F. Chen, J. L. Luo, N. L. Wang, J. Hu, and P. Dai, arXiv:0807.1077 (unpublished).
[25] See EPAPS Document No. E-PRBMDO-78-R10834 for a comparison between the measured and calculated structure factors for the magnetic peaks in the refinement. For more information on EPAPS, see http://www.aip.org/pubservs/epaps.html